

# Dynamics of carbon nanopillar growth on bulk and thin substrates irradiated by a focused electron beam

G.S.Zhdanov\*, A.D.Manukhova\*\* and M.S.Lozhkin\*\*\*

Saint-Petersburg State University, Saint-Petersburg, Russia

\*gshdanov@mail.ru, \*\*alisa.manukhova@spbu.ru, \*\*\*maksim.lozhkin@spbu.ru

## ABSTRACT

Factors affecting the growth rate and aspect ratio of nanopillars grown by electron beam induced deposition of carbon on various substrates are discussed. The growing pillar evolves from flattened disk or a spherical cap to a sharpened cone and saturates at 250-300 nm. The minimum tip radius measured on vertically grown tip is about 10 nm and is most likely determined by the escape length of secondary electrons from carbon.

**Keywords:** electron beam induced deposition, carbon nanopillars, surface diffusion, electron beam scattering

## 1 INTRODUCTION

Electron beam induced deposition (EBID) of various materials on substrates has a wide range of potential applications which attract growing interest [1]. Study of carbon deposition has the most extensive literature. Considerable effort is aimed at better understanding complicated electron-substrate-precursor interactions that affect formation of nanometer-size dots and pillars on substrates.

It is often argued that pillars grown on different substrates do not differ considerably when deposition conditions remain the same [2]. Our results indicate otherwise.

## 2 EXPERIMENT

Carbon nanopillars were created and studied using a Carl Zeiss Crossbeam 1540 XB dual beam instrument attached with a secondary ion mass-spectrometer (SIMS). Carbon containing molecules were dissociated by 20 keV electron beam focused to a spot of ~1 nm radius at beam currents 5-400 pA.

In most cases residual hydrocarbons were used as a precursor. SIMS reveals presence of n-alkanes with partial pressures in the  $10^{-8}$  –  $10^{-9}$  mbar range at total background pressure  $\sim 5 \times 10^{-7}$  mbar in the specimen chamber. An auxiliary hydrocarbon source placed at the specimen stage was used to increase deposition rate on silicon.

EBID of carbon was performed on various substrates including highly oriented pyrographite (HOPG), naturally oxidized silicon wafers, and amorphous carbon films, produced by arc evaporation of carbon rods onto cleaved KCl crystals. Films were detached from the substrate in water and picked up on copper grid.

Deposits were studied *in situ* in a scanning electron microscope (SEM) and then transferred to an atomic force microscope (AFM) for precise measurements of pillar height at the initial stage. Correction factors were introduced to compensate for distortion of feature dimensions along the beam axis on tilted SEM images.

## 3 RESULTS AND DISCUSSION

### 3.1 Precursor interaction with scattered electrons.

The volume growth rate  $dV/dt$  of carbon nanopillars on Si was  $\sim 3 \times 10^2 \text{ nm}^3 \text{ s}^{-1}$  which is insufficient to trace growth dynamics during acceptable exposure time. By using an auxiliary hydrocarbon source we could increase precursor molecular flux by a factor of 20-80. The sequence of SEM images obtained under these conditions at different exposure times are shown in Fig. 1.

EBID of carbon on freshly cleaved HOPG was performed in standard vacuum, however, high volume ( $dV/dt \sim 5 \times 10^5 \text{ nm}^3 \text{ s}^{-1}$ ) and vertical ( $dh/dt \sim 1-3 \times 10^2 \text{ nm s}^{-1}$ ) growth rates were registered during the first 100-500 ms of deposition [3]. After  $t \sim 10$  s the growth practically stops. The measured initial deposition rates exceed by a factor of  $\sim 10^5$  those expected by direct impingement of molecules from the gas phase onto the pillar apex.

These results prove high diffusivity of hydrocarbons on flat and initially clean HOPG surface. Assuming that all molecules traversing the irradiated area of radius  $\rho$  would be dissociated and polymerized, we obtain diffusion induced rate enhancement factor  $m \approx 2(\lambda/\rho)^2 / [\log(1.13\lambda/\rho)]$  where  $\lambda$  is diffusion length of molecules on an unexposed surface [3]. With reasonable  $\lambda \sim 10 \mu\text{m}$ ,  $\rho \sim 20 \text{ nm}$  (pillar base radius at the initial stage) one finds  $m \sim 10^5$  in accordance with the value mentioned above.

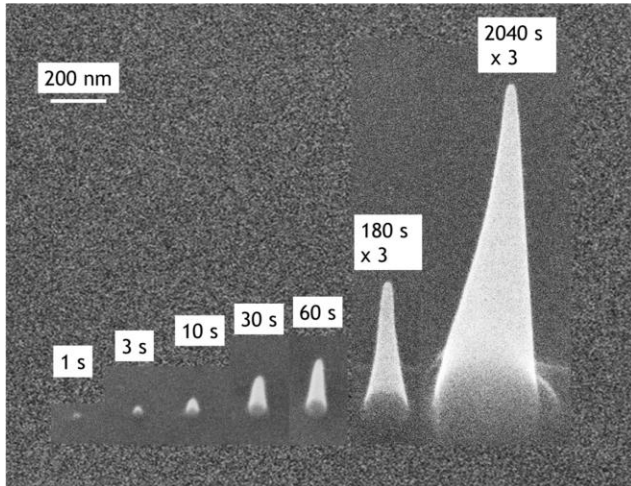


Figure 1: Successive stages of carbon nanopillar growth on Si,  $U=20$  kV,  $I=10$  pA. Two larger pillars were grown at deposition rate three times higher than the others to minimize shape distortion caused by the stage drift. An auxiliary hydrocarbon source was used to increase deposition rate on Si.

A dramatic fall of the deposition rate at the next stage might be due to interaction of adsorbed molecules with backscattered (BSE) and secondary (SE) electrons producing progressive contamination of initially clean surface. Indeed, ring-like  $\mu\text{m}$ -size contamination structures become visible after several minute exposure [3].

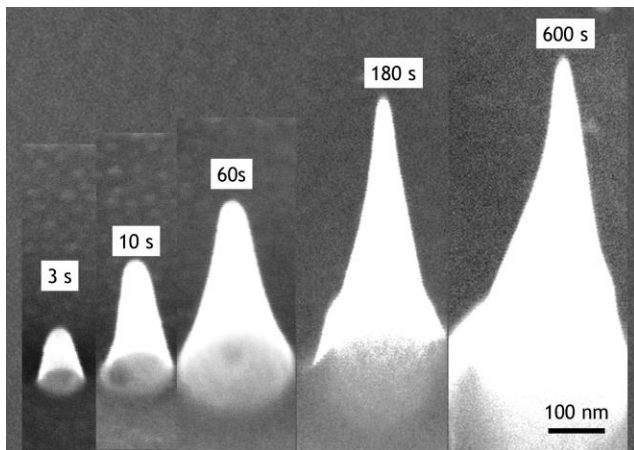


Figure 2: Successive stages of carbon nanopillar growth on the upper side of  $\sim 40$  nm thick amorphous carbon film,  $U=20$  kV,  $I=7$  pA. Depositions were performed without any complementary contamination sources.

To reduce the effects caused by BSE we performed deposition on thin amorphous carbon films with negligible

BSE yield. As expected, no substantial decrease of  $dV/dt$  with time was found at beam current of 7 pA, as illustrated by Fig.2. Of interest is that pillars grown on Si are narrower than pillars grown on amorphous carbon. It might be that impingement of molecules on the pillar side walls directly from an auxiliary source rather than by surface diffusion favors formation of tips with smaller cone angles.

At higher beam currents ( $I \sim 200$  pA) deposition on the two opposite sides of the thin substrate develops in different ways:  $dV/dt$  decreases with time and eventually falls off to zero on the upper side, while  $dV/dt \approx \text{const}$  on the lower side. As a result, pillars grown on the upper side became much smaller than their lower counterparts, as seen from Fig.3.

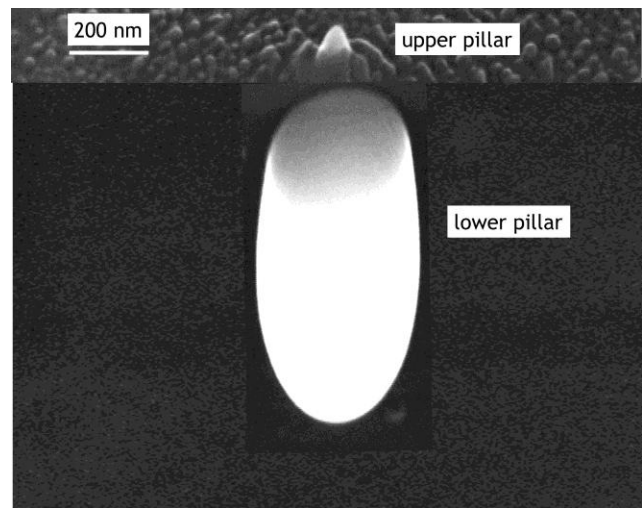


Figure 3: Carbon nanopillars grown on two opposite sides of 180 nm thick amorphous carbon film at 5min deposition,  $U=20$  kV,  $I=200$  pA. Note increased substrate roughness at the top.

Roughening of the upper side of the exposed film indicates contamination buildup probably induced by scattered electrons emitted from the pillar sidewalls. At the same time, the opposite side of the film apparently remains uncontaminated allowing pillar volume growth rates to be as high as  $5\text{-}8 \times 10^5 \text{ nm}^3 \text{ s}$  during all exposure time.

### 3.2. Evolution of the pillar profile.

As seen from Fig.1, pillars evolve from a spherical cap to a sharpened cone. The pillar height  $h$  and the base width  $w$  scale with exposure time  $t$  as  $h \sim t^\alpha$ ,  $w \sim t^\beta$  with  $\alpha + 2\beta \approx 1$ . Initially  $\alpha > \beta$  probably due to increased SE yield from the pillar side walls demonstrated via Monte Carlo simulation [4]. Extrapolation of the observed dependences to zero

time, demonstrated by plots in Fig.4, shows that the pillar “nuclei” should most probably resemble a flattened disk ( $w > h$ ) rather than a cone in agreement with data [5].

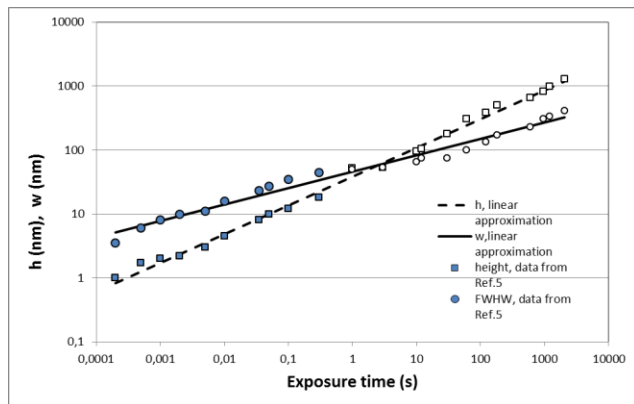


Figure 4: The pillar height  $h$  and the base width  $w$  on silicon vs the exposure time  $t$ , log-log scale. Data from ref.5 at small exposure times are used for comparison

### 3.3. Formation of nanopillar tip.

Intuitively, one might expect molecule deposition rate at the tip to be determined by primary electrons (PE) focused to a spot of  $\sim 1$  nm radius. These expectations are not confirmed experimentally. The smallest measured tip curvature radius is about 10 nm (see Fig.5) which is close to ultimate results obtained with other instruments at 20 kV by vertical growth [1]. Precise measurements are difficult due to contamination buildup during imaging mode. Still, the difference between the measured tip radius and the expected one highly exceeds possible distortions produced by side effects.

The most plausible explanation adopted by many authors (see [1, 2] for refs.) is that SE rather than primary electrons (PE) are responsible for precursor molecule dissociation near the pillar apex. In this case the pillar tip radius should be determined by SE escape length from carbon ( $\sim 10$  nm [6, 7]) rather than by current density distribution in the PE beam crossover.

Alternatively, one may come to the same conclusion comparing PE current densities at the beam incidence point and at the cone side walls at distance of about 200 nm from the tip. The latter is  $\sim 10^3$  times less than the former while the vertical and the lateral growth rates of carbon nanopillars are comparable.

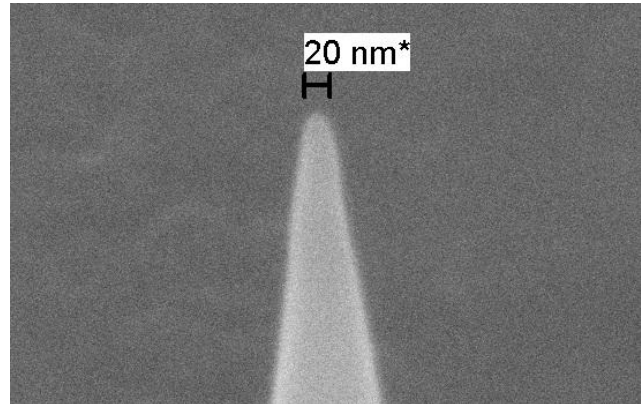


Figure 5: Image of a typical pillar tip taken at high magnification. As-grown pillar might be a little bit narrower since it expands laterally by 1-2 nm with each scan.

## 4 SUMMARY

Growth of carbon nanopillars proceeds differently on various substrates and, moreover, on opposite sides of the same substrate transparent for fast electrons. Surface diffusion of adsorbed precursor molecules seems to be one of the main factors determining the growth rate. Long-range effects caused by molecule interaction with back- and forward-scattered electrons at distances up to several micrometers from the beam incidence point might be responsible for dramatic variation of the growth rate with time.

EBID of carbon by 20 keV electrons allows fabrication of pillars of various shape and size ranging from about 10 nm to 10  $\mu$ m.

*We acknowledge the use of the facilities at the Resource Centre “Nanofabrication of Photoactive Materials (Nanophotonics)” of Saint-Petersburg State University. Two of us (Manukhova, Lozhkin) are grateful to OPTEC (Carl Zeiss Grant for young researchers, 2013) for financial support.*

## REFERENCES

- [1] I.Utke, S.Moskalev, P.Russell, “Nanofabrication Using Focused Ion and Electron Beams: Principles and Applications”, Oxford, 2012.

- [2] T.Bret “Physico-Chemical Study of the Focused Electron Beam Induced Deposition Process”, Thesis, Lausanne, EPFL,2005
- [3] G.S. Zhdanov, A.D. Manukhova et al., Bull. Russ. Acad. Sci. Phys., 77, 935, 2013.
- [4] N.Silvis-Cividjian, C.W.Hagen, P.Kruit , J. Appl. Phys., 98, 084905,2005.
- [5] O.Guise, J.Ahner, J.Yates, J.Levy , Appl.Phys.Lett., 85,2352,2004.
- [6] L.Reimer “Scanning Electron Microscopy and Microanalysis”, 2nd ed., Springer, Berlin, 1998
- [7] H.Seiler, J.Appl.Phys., 54, R1, 1983